Clinic Rev Bone Miner Metab (2016) 14:26–37
DOI 10.1007/s12018-015-9201-1

ASSESSMENT OF BONE HEALTH

FEA to Measure Bone Strength: A Review

Klaus Engelke[1] · Bert van Rietbergen[2] · Philippe Zysset[3]

Published online: 11 January 2016

Abstract Finite element analysis (FEA) based on CT datasets of the spine or hip or on high-resolution peripheral CT datasets of the distal forearm or tibia is now widely used in research and clinical trials to estimate bone strength. Its clinical potential has recently been endorsed by the International Society of Clinical Densitometry Zysset et al. (J Clin Densitom 18(3):359–92, 2015). In vitro validation studies demonstrated the superiority of FEA over DXA for the prediction of ultimate load. In vivo studies confirmed the superiority in the spine, but data were less conclusive in the hip and forearm. Here, in addition to low bone strength the risk of falling is a major determinant of fracture risk. The next level of FEA dissemination, the integration into clinical practice, still faces a number of challenges such as access to dedicated FE software and its integration into the clinical workflow. Also compared to DXA, current FEA techniques have not shown a consistent superiority for hip fracture prediction, while hip CT is associated with a higher radiation exposure than hip DXA. For many clinicians, FEA and the direct measurement of strength instead of BMD are a novel perspective. However, the increasing use of abdominal and pelvic CT scans initially obtained for other clinical diagnosis, for the secondary use to assess osteoporosis and fracture risk (opportunistic screening), may accelerate the use of FEA. In this contribution, the basic technical aspects and limitation of FEA are discussed and the clinically relevant outcome measures are presented. Further advanced topics will broaden the understanding of the various aspects of FEA. Afterward a summary of in vivo studies using FEA for fracture prediction is given, which also includes a discussion of the clinical value of FEA for bone strength measurements.

Keywords Finite element analysis · Bone strength · Hip · Spine · Forearm

✉ Klaus Engelke
klaus.engelke@imp.uni-erlangen.de

[1] Institute of Medical Physics, University of Erlangen, Erlangen, Germany

[2] Orthopedic Biomechanics, Department of Biomechanical Engineering, University of Eindhoven, Eindhoven, The Netherlands

[3] Institute for Surgical Technology and Biomechanics, University of Bern, Bern, Switzerland

Introduction

For several decades, areal bone mineral density (aBMD) has been the gold standard to assess fracture risk. Areal BMD as measured by dual X-ray absorptiometry (DXA) is the basis of the WHO operational definition of osteoporosis and is widely used to monitor age- and treatment-related changes. In vitro, there is a high correlation between aBMD [or vBMD as measured by quantitative computed tomography (QCT)] and bone strength as determined by mechanical testing with r^2 values between 0.6 and 0.8 [1–9]. However, the number of patients at risk needed to treat (NNT) to avoid one hip fracture is still about 30–70 [10, 11] with lower NNTs being reported for the spine [12–15]. Of course, there are many other risk factors in addition to BMD but eventually a bone fractures because it cannot sustain the external loads acting upon it. Therefore, a direct measurement of bone strength seems to be preferable to the measurement of densitometric parameters such as BMD.

So far, in vivo, a direct measurement of bone strength is not possible; however, strength can be estimated using the

finite element (FE) method, which is routinely used in mechanical engineering to calculate strength of complex structures under the action of external forces. During recent years, in vivo finite element analysis (FEA) applied to computed tomography (CT) scans has developed into a mature application to estimate bone strength of the hip, spine and distal radius. This was acknowledged by 2015 consensus positions of the International Society of Clinical Densitometry (ISCD) [16], which state that bone strength as estimated by FEA can be used for fracture prediction in postmenopausal women and elderly men and that the FE technique can also be used for monitoring of age- or treatment-related strength changes in the elderly population. The ISCD positions apply to FEA of spine and hip CT scans taken from whole-body clinical CT scanners. For CT scans of the forearm, typically dedicated high-resolution peripheral CT devices are used. State of the art of this approach and its related FE techniques were recently summarized in a review on FEA of the forearm [17].

Despite the advances in FE technology, all recent reviews [16–20] showed that currently the improvement in fracture prediction using strength-related variables instead of BMD is modest at best with the largest advantage being demonstrated in the spine. From a clinical perspective the use of FEA may still be questioned. Thus, this review will primarily address the question: What are benefits and limitations for a more widespread use of FEA in clinical practice? The recent exhaustive literature reviews of FE techniques [16–20] will serve as references but will not be repeated here. Nevertheless, a basic understanding of the FE technique is necessary for an adequate interpretation of the clinical results. In particular, there are different flavors of FEA, which affect clinical outcome, and an appreciation of their respective strengths and limitations is key for an assessment of the clinical value of FEA.

FE Technology

Basics

The main idea of FEA is to reduce a complicated mechanical problem, in this case the calculation of strength of a complex structure such as bone, to a set of algebraic equations. Specifically, a bone is divided into a number of small finite elements of a simple geometry for which deformations, stresses or even failure can be calculated easily. For this purpose, material properties of each of the elements need to be known. Under the requirement of an equilibrium of forces and moments for every element and the definition of these material properties, the mechanical response of a whole bone subjected to external forces can be calculated.

An engineering analog for the trabecular architecture of the vertebra is an old-fashioned steel bridge. External forces applied to the bridge, for example by the weight of a truck, cause elastic, reversible deformations of the steel bars such as bending and small changes in length. An increase in external forces eventually causes irreversible deformations and cracks that ultimately cause the failure of the bridge or the fracture of the bone. The analogy between the bridge and the trabecular structure presumes that the spatial resolution of the imaging technique is high enough to separate the individual trabeculae, so that the mesh of the finite elements represents the trabecular structure.

In this case, we talk of μFE. Typical applications are the investigation of trabecular bone samples imaged with μCT with spatial resolutions below approximately 40 μm. As discussed further below, μFE analysis can be applied in vivo at the distal forearm or tibia. In contrast, in the spine and hip, the spatial resolution achievable with whole-body clinical CT scanners is only around 0.5 mm and the segmentation of individual trabeculae is no longer possible. Instead, the measured CT values are calibrated to BMD; in essence, quantitative CT (QCT) is the basis of FEA at the spine and hip. These are the so-called homogenized FE models. A mesh is applied to the entire vertebral body or hip resulting in individual elements with a size in the millimeter range containing mineralized bone as well as bone marrow. The term homogenization denotes the averaging process used in determining the apparent material properties of the bone–marrow mixture, which are essential input parameters for FE analysis.

The outcome parameters of FEA are the same structural properties as the ones retrieved in biomechanical tests using cadaveric bones. The application of an external load to the bone causes a displacement at that location, and the progressions of these two variables in time produce a load–displacement curve (Fig. 1). The slope of the initial linear part of this curve, i.e., of the range of the elastic deformation is termed stiffness. The ultimate or failure load is the maximal load attained before the bone breaks. The energy to failure is the area under the curve. This load–displacement curve can also be simulated with FEA. The linear part of the curve, i.e., stiffness, can be obtained with linear FEA, while simulation of the yielding of the curve, the maximal force and the energy to failure requires nonlinear FEA. For in vivo measurements, estimated failure load reported typically in kN is the most widely used parameter and is often reported as bone strength not to be confused with ultimate stress, which is a material variable (Table 1; Fig. 1).

Structural properties such as stiffness, failure load and energy to failure depend on bone size. Normalizing displacement by length, failure load by area, and energy by volume results in material variables called strain, stress and energy density (Table 1; Fig. 1). Instead of a load–

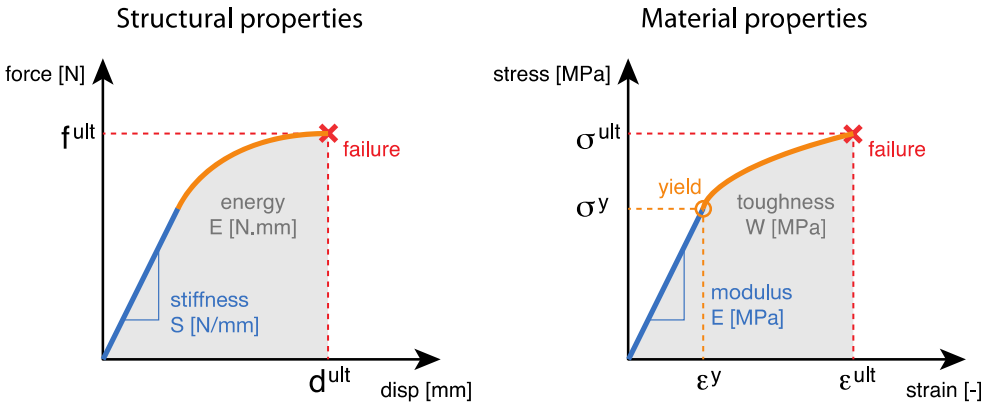

Fig. 1 Comparison of structural and material properties. Structural properties depend on size, while material properties normalize displacements by length into strains, forces by area into stresses and energy by volume into energy density. Structural properties are the principal outcome variables, while material properties are the necessary input variables for finite element analysis

Table 1 Typical parameters used in FEA analysis; see also Fig. 1

	Structural properties Extrinsic parameters	Material properties Intrinsic parameters
What is simulated by FEA?	External force F or load (N)	External stress = F/A (N/mm^2)
Main endpoint (unit)	Ultimate or fracture load (N)	Ultimate strength (N/mm^2)
	f^{ult} in Fig. 1	σ^{ult} in Fig. 1
Secondary endpoint (unit)	Stiffness (N/mm)	Young's modulus (MPa)
	S in Fig. 1	E in Fig. 1
Bone size dependent?	Yes	No
Typical application	Continuum FEA applied in vivo to hip and spine	μFEA applied to bone specimen or in vivo to the distal radius

displacement curve, a stress–strain curve is obtained that is independent of sample shape and size. The slope of the linear portion of the stress–strain curve is Young's modulus. The maximum stress at which the bone breaks is termed ultimate stress, and the energy density to failure is called toughness. Young's modulus, ultimate stress and toughness are therefore (intrinsic) material properties, independent of shape and size. In fact, these variables are the material properties needed as input for FEA and are determined in ex vivo biomechanical tests of compact or trabecular bone samples with regular shapes.

The same normalization idea can also be applied to FEA output variables for bones with regular shapes such as radial or vertebral sections. The ultimate force can be divided by the average cross-sectional area providing an ultimate stress that may be more meaningful in terms of fracture risk because it takes the size of the bone into account. Unfortunately, this normalization cannot be applied to bones with irregular shapes such as the proximal femur.

Advanced Topics

Material Properties: Trabecular—Cortical Bone

Bone tissue is a quasi-brittle, heterogeneous and anisotropic material that deforms elastically under small strains and exhibits a microcracking mechanism resulting in the simultaneous accumulation of irreversible strains and the reduction of the original elastic modulus when deformed beyond yield strains of approximately 0.3–0.4 % [21, 22]. This material behavior holds for compact and trabecular bone, as both are constituted of lamellar bone tissue. In practice, bone is modeled as a linear elastic material (linear material law) that may lead to plasticity or damage beyond a given yield criterion (nonlinear material laws) [23]. Beyond yielding, the material behavior is modeled with some strain hardening or softening function that mimics the increasing or decreasing post-yield stresses observed in experiments. The various material models are then characterized by material constants such as Young's modulus, yield stress or ultimate stress and linear hardening slope.

The actual material constants of compact bone are dominated by porosity and Haversian orientation [24], while the ones of trabecular bone are almost entirely controlled by bone volume fraction (BV/TV) and architectural anisotropy also called fabric [25]. X-ray attenuation exploited in computer tomography is well suited to quantify bone volume fraction and to a certain degree porosity, but Haversian orientation and trabecular fabric depend on image resolution and cannot be easily assessed in vivo.

In μCT-based FE or μFE (≤40 μm), bone tissue properties are generally assumed to be homogeneous and

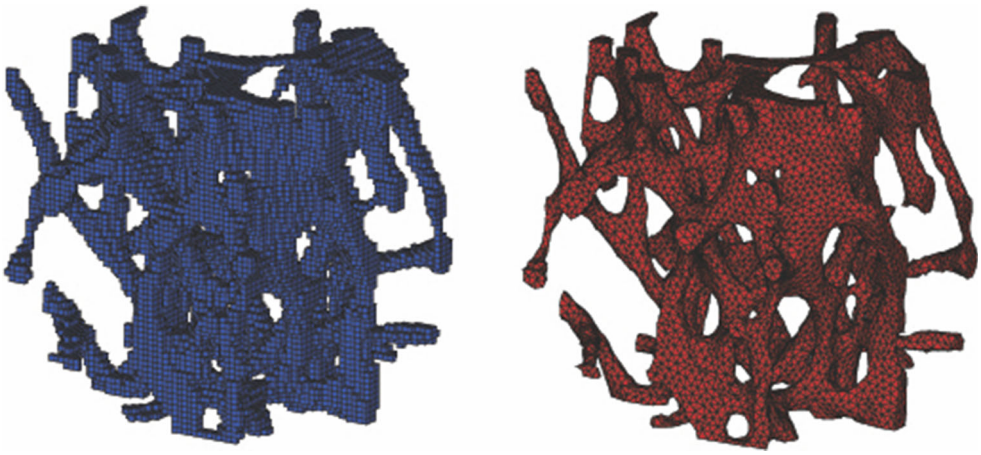

Fig. 2 μFE model resolving the trabecular microstructure. The mesh can be voxel-based or smooth. The bone tissue is usually assumed homogeneous

isotropic, which is justified by the fact that mineralization has a narrow range [26, 27] and that trabeculae are principally loaded along their length in compression, bending or torsion. In high-resolution peripheral CT of the distal radius or tibia (60–80 μm), the vascular and resorption space contributions to cortical porosity can be resolved and trabecular architecture can be estimated [28]. However, the actual bone volume fraction is often overestimated in μFE and homogenized FE is an attractive alternative for these spatial resolutions as well [29].

In whole-body QCT of the vertebral body or proximal femur (300–500 μm), Haversian orientation and fabric are hardly detectable, porosity and volume fraction can be estimated from local BMD, and homogenized FE is the only option. At these resolutions, compact and trabecular bone are often not distinguished and the material properties are assumed isotropic. In the vertebral body, principal trabecular orientation is sometimes assumed to run along the cranio-caudal direction [30], while in the femur, registration or machine learning tools are currently explored to retrieve the fabric information indirectly from a given anatomical database [31–33]. Material property mapping, the assignment of material properties to each element using the underlying CT image, is an important feature of homogenized FE models [34, 35]. FE outcome measures somewhat depend on whether the mapping is performed voxel by voxel, interpolated from a virtual grid or averaged over a specific volume [34].

Meshing Techniques

In computational engineering practice, mesh generation is a time-consuming task, which explains the attractiveness of voxel meshes that automatically convert voxels coarsened from a CT image into finite elements (Fig. 2). The main disadvantages of voxel meshes are the irregular boundaries and the lack of refinement at locations where failure occurs. Alternatively, marching tetrahedron meshing options have been developed that can mesh the models with tetrahedron elements and have smooth boundaries, but typically these meshes use only one element size and thus may contain many elements. More general hexahedral or tetrahedral meshes require more effort, can be only partly automated, offer smooth boundaries and can be refined where needed [36]. Moreover, these meshes offer the possibility to model distinctly the compact shell and the trabecular core of whole bones (Fig. 3).

Linear Versus Nonlinear FEA

Linear FEA considers only the elastic behavior of the bone matrix and assumes that only small strains and rotations occur in the structure. Nonlinearity of the computational problem may be introduced from a geometrical or material point of view. Bending of a slender linear elastic beam results in a geometrical nonlinearity, while the microcracking mechanism of bone tissue represents a material nonlinearity. Nonlinear material properties are necessary to simulate loading beyond the yield point, reach an ultimate load and describe the permanent displacements and reduction in stiffness appearing after unloading.

Nonlinear FEA exploits linear iterative methods that convert the nonlinear numerical problem into a sequence of linear problems and requires therefore approximately an order of magnitude longer computing time for each load step. Unlike linear analyses, nonlinear analyses necessitate multiple load steps to ensure convergence of the iterative method, which results into even larger differences in computing time. Since computing time is also a power function of the number of elements, nonlinear analyses of large μFE models reach the limits of standard computational resources and require computing clusters or high-performance computer centers.

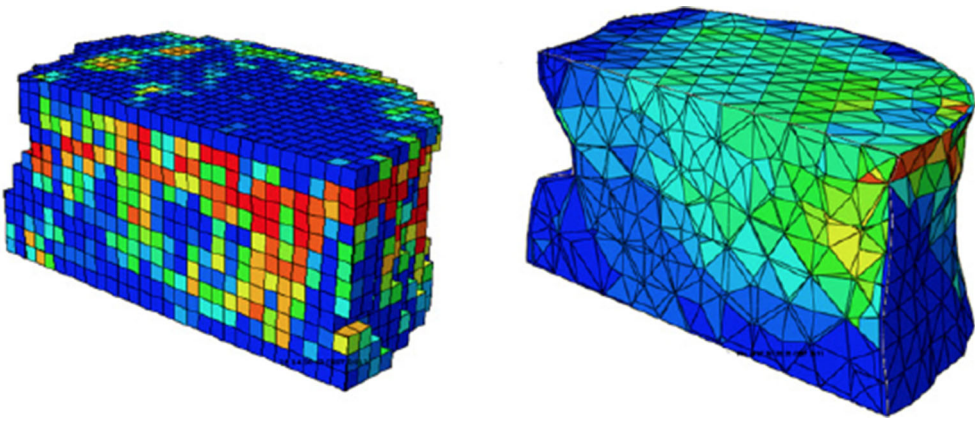

Fig. 3 Voxel and a smooth meshes of a vertebral body section for homogenized FE adapted from [78]. The *color map* designates bone volume fraction (BV/TV) (Color figure online)

Definition of Failure Criteria

Failure criteria allow to estimate bone strength and to predict the anatomical locations where failure is initiated and progresses. They also play a central role in FE validation in biomechanical experiments.

In linear FE analysis, force–displacement curves are linear and do not reach a maximum to determine ultimate force. Consequently, failure criteria are generally computed from the strain distribution as stresses scale with material properties and no plastic or damage variables are calculated. A typical definition is the fraction of bone tissue that exceeds a given strain level [37]. For instance, in μFE analysis of the distal radius, the so-called Pistoia criterion defines the force where 2 % of the tissue exceeds an effective strain of 0.007 [38]. Such definitions depend on bone geometry, mesh, material properties and load case and must be interpreted carefully.

In nonlinear FEA, the actual maximum of force–displacement curves can be simulated and is therefore the preferred outcome [39]. However, the computed ultimate load depends on the yield criterion and the hardening properties selected at the material level [40]. With a few exceptions, most of the yield criteria used for bone have been borrowed from other engineering materials without further validation. The sensitivity of ultimate load to these criteria has been investigated with mixed results that reflect the limitations of the FE models and the related experiments [41]. Nevertheless, strain measures are currently favored, a distinct criterion in tension and compression is meaningful, and the compressibility of trabecular bone yielding was demonstrated in several studies [42, 43].

Validation

FE methods have been validated in numerous experimental studies using cadaveric bones. Correlations (r^2) between estimated and measured failure loads or ultimate strength ranged from 0.78 to 0.96 in the spine, from 0.85 to 0.9 in the hip (see [19] for a summary) and from 0.66 to 0.94 in the distal radius (Table 2). When directly comparing FE simulations with BMD or BMC as measured by DXA or QCT, at the radius, spine and hip FE parameters in general correlated higher with experimental

Table 2 Overview of validation studies for μFE using HR-pQCT

Experimental test region	*n*	Voxel size (μ)	Boundary conditions	Tissue Young's modulus (GPa)	Failure criterion	r^2	Slope	Ref
Intact forearm	54	165	High friction	10	Pistoia	0.66	0.73	[46]
Intact forearm	100	89/93	Low friction	6.83	Pistoia	0.73	–	[48]
					Adapted Pistoia	0.73	–	
	20			$6.85\rho^{1.5}$	Nonlinear	0.82		
Distal radius XtremeCT scan region	5	82	Low friction	6.82	Nonlinear	0.94	0.95	[60]
				$15\rho^{1.7}$		0.95	1.82	
Excised distal radius	21	82	High friction	15	Pistoia	0.92	1.03	[47]

ρ bone mineral density

measures than with aBMD. Differences between FE and QCT parameters were smaller, but FE correlations were still slightly higher. However, it is important to note that the structural variable of failure load should be compared with BMC or a size-adjusted vBMD measure, whereas the material variable ultimate strength should be compared with vBMD and not with BMC.

In the hip, failure load estimated by FEA also correlated higher with the experimental measurement than aBMD or BMC. Thus, when just considering the external forces acting on bone, strength parameters are better predictors of fracture than surrogate QCT or DXA BMD or BMD measurements. The combination of BMD or BMC with geometrical parameters such as cortical thickness, which in the hip in vivo has shown improved fracture prediction over vBMD alone [44], has not been tested for failure load prediction in vitro. However, the combination of multiple parameters to predict fracture requires a multivariate analysis and is more difficult to interpret than a single parameter such as ultimate load.

A validation of forearm μFE results was performed in several studies using cadaver arms [45–48]. Most of these studies also included DXA scans of the distal forearm. μFE and experimental results were highly correlated, with a coefficient of determination $r^2 > 0.66$ (Table 2). The accuracy depended on the accuracy of the experimental test (intact forearm testing is not very accurate) and on the material properties chosen, which varied widely among studies. When using accurate tests and tuned tissue material properties, however, highly accurate results were obtained [45, 47]. Interestingly, in all these studies μFE better predicted bone strength than DXA, although in some of these studies the improvement was rather small.

Precision of FE Parameters

Reproducibility of the FEA outcome variables primarily depends on the reproducibility of the CT or other images on which the models are based. In vivo root-mean-square precision errors of advanced QCT or HR-pQCT analyses techniques are comparable to DXA: 1–2 % for integral BMD in the total vertebral bodies of the lumbar spine [49, 50], total hip [51–54] and distal forearm [55, 56]. For FEA a precision error of 1.9 % for total hip stiffness was reported [57]. Due to the use of local BMD values in bone segmentation and in the assignment of material properties, the original QCT precision will be degraded in a resolution-dependent manner along the FE model production and execution pipeline. A recent study suggests that femoral strength computed by linear FE in a fall configuration has a CV of 6.4 % compared to the one of a nonlinear FE in a stance configuration with a CV of 1.6 %.

The short-term reproducibility of the μFE results was reported in several studies [58–60], in which a group of subjects was scanned twice or thrice at different days or after repositioning. Typically, root mean square of the coefficient of variation was better than 4.4 % for stiffness and 3.7 % for strength, which are values comparable to the reproducibility of the microstructural parameters.

Clinical Use of FE Techniques

The application of FEA in the bone field is still a topic of ongoing research activities, and many studies were carried out with university-based experimental software. So far, for spine and hip FEA software is not available off the shelf although a number of companies offer services for data analysis. Among them ON-Diagnostics' (Berkeley, CA) VirtuOst software and its predecessors have been used for the analysis of epidemiological studies and of many clinical studies to develop new pharmaceutical drugs to prevent fractures. VirtuOst has been recently approved by the FDA. Likewise, FEA of the forearm has been mostly performed by university-based software. An FEA analysis option for HR-pQCT scans of the distal radius and tibia has been integrated into the analysis software installed on the XtremeCT scanners (Scanco Medical, Brüttisellen, Switzerland). In the next two sections, state-of-the-art in vivo FEA at the forearm using HR-pQCT scanners and at the spine and hip using whole-body clinical CT scanners will be summarized.

FEA of Spine and Hip

Spine and hip are the most important fracture sites. One focus of FEA (Fig. 4) is the necessity to improve fracture prediction and to more accurately identify subjects at high risk in whom treatment is highly indicated. From a clinical perspective, the main questions are: Is FEA more accurate than DXA, what is the additional effort and will it benefit the patient? First, there are a number of logistical issues. As described above access to FE technology in particular for spine and hip is still limited. In addition, a QCT dataset is a prerequisite for FEA. While there are probably more clinical whole-body CT scanners than DXA scanners, historically physicians treating osteoporosis have easier access to DXA. Finally, there is the issue of radiation exposure that is considerably higher for CT than for DXA: about 1 mSv effective dose for QCT of two lumbar vertebrae and 2–3 mSv for a total hip scan compared to about 5 μSv each for DXA of the lumbar spine and total hip. On an absolute scale, radiation exposure for QCT is rather low, approximately equivalent to the annual background radiation and the benefit may largely outweigh the potential

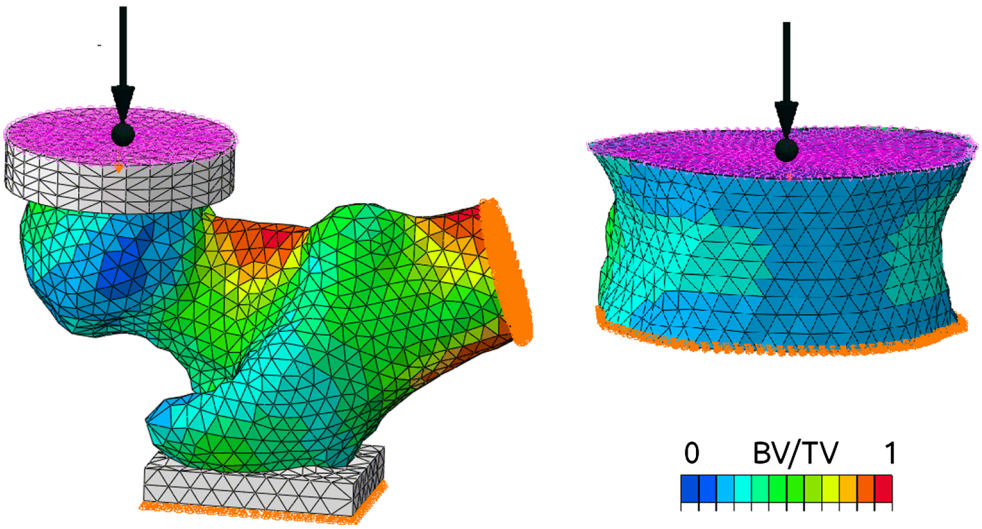

Fig. 4 Two examples of boundary value problems resolved with the FE method. Loading of the proximal femur in a side fall configuration and axial compression of a vertebral body section. Adapted from [79]. The *color map* designates bone volume fraction (BV/TV) (Color figure online)

risks, in particular in elderly people, where osteoporosis is of major concern. However, if the benefits of a QCT or FE analysis do not outweigh those of DXA then there is no rationale to perform a CT scan. So how do the techniques compare with respect to fracture prediction?

The most solid data to date were generated from two epidemiological studies: MrOs a US study in elderly men and Ages Reykjavik an Icelandic study in elderly females. In a subcohort of the MrOs study, standardized HRs were higher for failure load of L2 than for DXA aBMD of L1–L4 [61], and in a subcohort of the Ages Reykjavik study, ORs were higher for strength of L2 than for vBMD of L2 [20]. In comparison with aBMD of the spine, two other studies in women showed either larger AUC values or higher correlations of strength parameters for discrimination of vertebral fractures [62, 63]. With respect to the hip, standardized HRs in the MrOs study were higher for hip failure load than for DXA hip aBMD [64]. Several cross-sectional studies in women showed that the power of FEA-derived strength measures to discriminate hip fractures was comparable to aBMD or vBMD measures of the total femur [20, 65, 66].

Thus, in vivo 'FEA of the spine was superior to DXA spine aBMD and superior or equivalent to QCT spine vBMD/BMC to predict failure load of the vertebral body. FEA of the hip was superior or equivalent to DXA hip aBMD and superior to QCT hip vBMD/BMC to predict failure load of the hip' [1]. In particular, in the spine, in vivo and in vitro data show a consistent superiority of vertebral facture prediction or discrimination of FEA strength measures but also of QCT BMC or BMD compared to aBMD as measured by DXA. The main reason is the 3D imaging technique of QCT and FEA that allows for a separate analysis of the vertebral body, unaffected by the spinous and transversal processes, the pedicles and potential aortic calcifications that falsely contribute to vertebral aBMD as measured in the projectional DXA technique. In addition, degenerative changes frequently observed in the elderly can more easily be omitted from the QCT/FEA than from the DXA analysis. These limitations of DXA that typically falsely increase aBMD in the spine have been known for a long time, but appropriate 3D imaging techniques were only developed after the invention of spiral CT.

In the hip differences are smaller. Even in vitro, the difference in correlations between estimated and experimentally measured failure load and between aDXA and experimentally measured failure load was much smaller than in the spine [19]. This translates to the in vivo situation where ultimate load by FEA of the hip improved fracture prediction only marginally compared to aBMD [20, 64, 65, 67]. Further, reported confidence intervals for hazard or odds ratios from FEA calculations are usually considerably larger than those from DXA. Therefore, even larger reported numerical differences among techniques may not have achieved statistical significance. The hip differs from the spine because hip DXA is not affected by the same limitations as spine DXA. Hip DXA is affected by the rotation of the leg, and the acetabulum often overlaps the most proximal part of the femur. Thus, in DXA only part of the neck is included in the analysis, whereas in QCT/FEA often a smaller part of the intertrochanteric region is included in the total femur VOI. Nevertheless, the analyzed total hip VOI is very similar between QCT/FEA and DXA.

However, the most important reason that in vivo FEA and aBMD still give very similar results in the hip is the fact that hip fracture is almost exclusively caused by a fall and the risk of falling is captured by neither DXA, QCT nor FEA. Thus, in particular in the hip in vitro experiments do

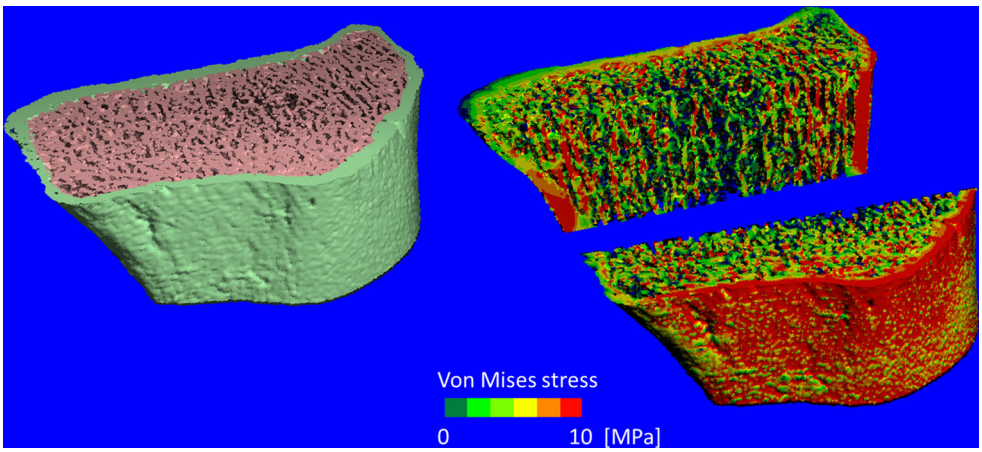

Fig. 5 *Left* a typical μFE model of the scanned section of the distal radius with the cortical bone tissue *colored green* and the cancellous bone tissue *pink*. *Right* the von Mises stress in the bone tissue for a 1 % compressive loading of the segment. The section is cut into two parts to reveal the stresses in the trabeculae (Color figure online)

not fully reflect the in vivo situation, although the part related to bone strength can be better captured by FEA than by DXA. Nevertheless, when following the argumentation at the beginning of the section, in the hip the use of CT instead of DXA may be questioned potentially limiting the use of FEA. However, many CT scans are routinely taken for other diagnostic purposes than for osteoporosis. Examples are standard abdominal or pelvic CT scans. Their potential in the diagnosis of osteoporosis or for the identification of high-risk fracture groups is currently being explored. These approaches are summarized as opportunistic screening [68, 69].

In short, existing clinical CT scans even those with contrast applications are 'externally' calibrated to BMD, i.e., using phantom scans obtained separately from the patient scan or are calibrated internally using air and soft tissues such as fat. Some researchers even suggest using the CT values directly [70, 71]. Then with appropriate thresholds, obtained, for example, in a comparative DXA study, DXA T-score equivalent thresholds for the diagnosis or at least for a rough stratification in high, normal, low fracture risk can be made. Obviously, this is not a diagnosis of osteoporosis in accordance with the WHO criteria but an alternative attractive risk stratification. Whether patients identified as being at high fracture risk according to this scenario will then undergo an additional DXA scan or not is still under debate. Of course, QCT as well as FEA parameters can be obtained with such an approach using existing data. Failure load of hip and spine could be a secondary outcome to other CT-based diagnoses. While first very promising results have been published [68], many methods related questions in particular with respect to the standardization of the CT acquisition and calibration process have to be answered. Nevertheless, this is a very promising approach to make FEA widely available in clinical routine.

FEA of the Forearm

The forearm is the third major fracture site for osteoporotic patients. Typically, these fractures occur as the result of a fall from standing height in subjects that are still capable to stretch out their hand to soften the fall. Although it is a major osteoporotic fracture site, the forearm is not a common site for DXA measurement or strength assessment by FEA. For research studies, however, this has changed with the introduction of HR-pQCT imaging around a decade ago. This technique enabled the imaging of the distal radius in vivo at a resolution that is high enough to resolve the bone microstructure (isotropic voxel size of 82 μm), thus offering a unique opportunity for microstructural and μFE analyses in patient studies (Fig. 5).

The radiation exposure for such measurements is around 3 μSv effective dose, which is comparable to a DXA scan and very low compared to a spine or hip CT scan. Since presently only one manufacturer is producing this type of equipment and only 2 models are available, the scanning procedure and microstructural and μFE analyses are highly standardized. The FE analysis can be performed in a fully automated manner, without any user intervention, making it highly suitable for clinical applications. For the μFE analyses, the images are usually first filtered and thresholded, after which each bone voxel is converted to a brick element. Then, a compression test is simulated on the scanned section, from which the stiffness of the section, the strength (estimated using the 'Pistoia criterion' mentioned earlier, or by performing a nonlinear analyses) and the distribution of the load between the cortical and cancellous compartment are calculated.

As discussed above, the validation studies showed that μFE analyses better predicted forearm bone *strength* than DXA, but it remains to be proven that it can better predict bone *fracture risk* [17]. In several retrospective studies, the

association between prevalence of a distal radius fracture and μFE or DXA results was quantified by odds ratios per standard deviation change. In postmenopausal women, odds ratios for μFE results generally were about the same as those for forearm DXA [72–74]. Interestingly, some studies indicated that biomechanical properties of the distal radius and tibia, based on in vivo HR-pQCT images, were associated with all types of fractures, including spine and hip, and were partially independent from hip aBMD [75, 76]. This suggests that microstructural changes at the distal radius might be representative for other sites as well and might provide additional information about the strength at other sites.

Nevertheless, to date, μFE and DXA give very similar results with respect to forearm fracture discrimination. As with the hip, the most important reason for this is probably the fact that forearm fractures are almost exclusively caused by a fall. It should be noted, however, that all fracture risk studies were retrospective studies, in which the fracture could have occurred more than a decade before the HR-pQCT scan was made, and in which the patients had been pharmaceutically treated since the fracture. Thus, the bone microstructure used for the μFE analyses might not have been representative for that during the fracture. Clearly, prospective studies are needed to better evaluate whether μFE can improve upon fracture risk prediction of the distal radius or even other sites. It should also be noted that all studies mentioned above were performed using the first generation of HR-pQCT devices. A second-generation device that offers 61 μm isotropic voxel size has just become available and was shown to provide an improved assessment of bone microstructure [77]. Although no bone strength studies have been reported using this device yet, it is possible that the increase in image resolution will further improve the strength assessment.

Conclusion

Despite the limitations listed above, FE is currently the most accurate method to estimate bone strength when a QCT reconstruction is available. This makes it the tool of choice for the evaluation of treatments aiming at increasing bone strength.

Since bone strength is only part of the fracture risk equation, the clinically added value of the improved accuracy in terms of fracture risk and the related gradient remains to be determined more accurately for each anatomical site.

Exploitation of opportunistic CT scans seems to be an attractive approach to screen for high fracture risk in our aging populations with minimal costs and to disseminate FEA more widely in clinical routine.

Knowledge of the underlying bone matrix mechanics, of the CT imaging procedure and calibration, of segmentation and meshing tools and of numerical algorithms is constantly improving. Thus, the FE method has the potential to estimate bone strength with an even higher accuracy. By intelligent combination of FEA with other risk factors, this should further improve the clinical assessment of fracture risk.

Compliance with Ethical Standards

Conflict of interest Bert van Rietbergen is a consultant for Scanco Medical AG. Klaus Engelke is a part time employee of BioClinica, Inc. Philippe Zysset has no conflict of interest.

Human and Animal Rights This is a review article. Studies with human or animal subjects were not specifically performed for the purpose of this article by any of the author.

References

1. Baum T, Kutscher M, Muller D, Rath C, Eckstein F, Lochmuller EM, Rummeny EJ, Link TM, Bauer JS. Cortical and trabecular bone structure analysis at the distal radius-prediction of biomechanical strength by DXA and MRI. J Bone Miner Metab. 2013;31(2):212–21.
2. Bjarnason K, Hassager C, Svendsen OL, Stang H, Christiansen C. Anteroposterior and lateral spinal DXA for the assessment of vertebral body strength: comparison with hip and forearm measurement. Osteoporos Int. 1996;6(1):37–42.
3. Hudelmaier M, Kuhn V, Lochmuller EM, Well H, Priemel M, Link TM, Eckstein F. Can geometry-based parameters from pQCT and material parameters from quantitative ultrasound (QUS) improve the prediction of radial bone strength over that by bone mass (DXA)? Osteoporos Int. 2004;15(5):375–81.
4. Imamoto K, Hamanaka Y, Yamamoto I, Niiho C. Correlation between the values of bone measurements using DXA, QCT and USD methods and the bone strength in calcanei in vitro. Kaibogaku Zasshi. 1998;73(5):509–15.
5. Lochmuller EM, Muller R, Kuhn V, Lill CA, Eckstein F. Can novel clinical densitometric techniques replace or improve DXA in predicting bone strength in osteoporosis at the hip and other skeletal sites? J Bone Miner Res. 2003;18(5):906–12.
6. Taton G, Rokita E, Wrobel A, Korkosz M. Combining areal DXA bone mineral density and vertebrae postero-anterior width improves the prediction of vertebral strength. Skeletal Radiol. 2013;42(12):1717–25.
7. Lochmuller EM, Lill CA, Kuhn V, Schneider E, Eckstein F. Radius bone strength in bending, compression, and falling and its correlation with clinical densitometry at multiple sites. J Bone Miner Res. 2002;17(9):1629–38.
8. Muller ME, Webber CE, Bouxsein ML. Predicting the failure load of the distal radius. Osteoporos Int. 2003;14(4):345–52.
9. Wu C, Hans D, He Y, Fan B, Njeh CF, Augat P, Richards J, Genant HK. Prediction of bone strength of distal forearm using radius bone mineral density and phalangeal speed of sound. Bone. 2000;26(5):529–33.

10. Johansson H, Kanis JA, Oden A, Johnell O, McCloskey E. BMD, clinical risk factors and their combination for hip fracture prevention. Osteoporos Int. 2009;20(10):1675–82.
11. Stewart A, Calder LD, Torgerson DJ, Seymour DG, Ritchie LD, Iglesias CP, Reid DM. Prevalence of hip fracture risk factors in women aged 70 years and over. QJM. 2000;93(10):677–80.
12. Black DM, Cummings SR, Karpf DB, Cauley JA, Thompson DE, Nevitt MC, Bauer DC, Genant HK, Haskell WL, Marcus R, Ott SM, Torner JC, Quandt SA, Reiss TF, Ensrud KE. Randomised trial of effect of alendronate on risk of fracture in women with existing vertebral fractures. Fracture intervention trial research group. Lancet. 1996;348(9041):1535–41.
13. Cummings SR, Black DM, Thompson DE, Applegate WB, Barrett-Connor E, Musliner TA, Palermo L, Prineas R, Rubin SM, Scott JC, Vogt T, Wallace R, Yates AJ, LaCroix AZ. Effect of alendronate on risk of fracture in women with low bone density but without vertebral fractures: results from the fracture intervention trial. JAMA. 1998;280(24):2077–82.
14. Harris ST, Watts NB, Genant HK, McKeever CD, Hangartner T, Keller M, Chesnut CH 3rd, Brown J, Eriksen EF, Hoseyni MS, Axelrod DW, Miller PD. Effects of risedronate treatment on vertebral and nonvertebral fractures in women with postmenopausal osteoporosis: a randomized controlled trial. Vertebral efficacy with risedronate therapy (VERT) study group. JAMA. 1999;282(14):1344–52.
15. McClung MR, Geusens P, Miller PD, Zippel H, Bensen WG, Roux C, Adami S, Fogelman I, Diamond T, Eastell R, Meunier PJ, Reginster JY, Hip G. Intervention program study, effect of risedronate on the risk of hip fracture in elderly women. Hip Intervention Program Study Group. N Engl J Med. 2001;344(5):333–40.
16. Zysset P, Qin L, Lang T, Khosla S, Leslie WD, Shepherd JA, Schousboe JT, Engelke K. Clinical use of quantitative computed tomography-based finite element analysis of the hip and spine in the management of osteoporosis in adults: the 2015 ISCD official positions-Part II. J Clin Densitom. 2015;18(3):359–92.
17. van Rietbergen B, Ito K. A survey of micro-finite element analysis for clinical assessment of bone strength: the first decade. J Biomech. 2015;48(5):832–41.
18. Engelke K, Libanati C, Fuerst T, Zysset P, Genant HK. Advanced CT based in vivo methods for the assessment of bone density, structure, and strength. Curr Osteoporos Rep. 2013;11(3):246–55.
19. Zysset PK, Dall'ara E, Varga P, Pahr DH. Finite element analysis for prediction of bone strength. Bonekey Rep. 2013;2:386.
20. Kopperdahl DL, Aspelund T, Hoffmann PF, Sigurdsson S, Siggeirsdottir K, Harris TB, Gudnason V, Keaveny TM. Assessment of incident spine and hip fractures in women and men using finite element analysis of CT scans. J Bone Miner Res. 2014;29(3):570–80.
21. Keaveny TM, Wachtel EF, Guo XE, Hayes WC. Mechanical behavior of damaged trabecular bone. J Biomech. 1994;27(11):1309–18.
22. Zysset PK, Curnier A. A 3D damage model for trabecular bone based on fabric tensors. J Biomech. 1996;29(12):1549–58.
23. Schwiedrzik JJ, Zysset PK. The influence of yield surface shape and damage in the depth-dependent response of bone tissue to nanoindentation using spherical and Berkovich indenters. Comput Methods Biomech Biomed Eng. 2015;18(5):492–505.
24. Martin RB, Ishida J. The relative effects of collagen fiber orientation, porosity, density, and mineralization on bone strength. J Biomech. 1989;22(5):419–26.
25. Maquer G, Musy SN, Wandel J, Gross T, Zysset PK. Bone volume fraction and fabric anisotropy are better determinants of trabecular bone stiffness than other morphological variables. J Bone Miner Res. 2015;30(6):1000–8.
26. Gross T, Pahr DH, Peyrin F, Zysset PK. Mineral heterogeneity has a minor influence on the apparent elastic properties of human cancellous bone: a SRmuCT-based finite element study. Comput Methods Biomech Biomed Eng. 2012;15(11):1137–44.
27. Roschger P, Gupta HS, Berzlanovich A, Ittner G, Dempster DW, Fratzl P, Cosman F, Parisien M, Lindsay R, Nieves JW, Klaushofer K. Constant mineralization density distribution in cancellous human bone. Bone. 2003;32(3):316–23.
28. Laib A, Hildebrand T, Hauselmann HJ, Ruegsegger P. Ridge number density: a new parameter for in vivo bone structure analysis. Bone. 1997;21(6):541–6.
29. Varga P, Zysset PK. Assessment of volume fraction and fabric in the distal radius using HR-pQCT. Bone. 2009;45(5):909–17.
30. Chevalier Y, Pahr D, Zysset PK. The role of cortical shell and trabecular fabric in finite element analysis of the human vertebral body. J Biomech Eng. 2009;131(11):111003.
31. Marangalou JH, Ito K, Cataldi M, Taddei F, van Rietbergen B. A novel approach to estimate trabecular bone anisotropy using a database approach. J Biomech. 2013;46(14):2356–62.
32. Marangalou JH, Ito K, van Rietbergen B. A novel approach to estimate trabecular bone anisotropy from stress tensors. Biomech Model Mechanobiol. 2015;14(1):39–48.
33. Lekadir K, Hazrati-Marangalou J, Hoogendoorn C, Taylor Z, van Rietbergen B, Frangi AF. Statistical estimation of femur microarchitecture using optimal shape and density predictors. J Biomech. 2015;48(4):598–603.
34. Marangalou JH, Eckstein F, Kuhn V, Ito K, Cataldi M, Taddei F, van Rietbergen B. Locally measured microstructural parameters are better associated with vertebral strength than whole bone density. Osteoporos Int. 2014;25(4):1285–96.
35. Pahr DH, Zysset PK. From high-resolution CT data to finite element models: development of an integrated modular framework. Comput Methods Biomech Biomed Eng. 2009;12(1):45–57.
36. Viceconti M, Bellingeri L, Cristofolini L, Toni A. A comparative study on different methods of automatic mesh generation of human femurs. Med Eng Phys. 1998;20(1):1–10.
37. Keyak JH, Fourkas MG, Meagher JM, Skinner HB. Validation of an automated method of three-dimensional finite element modelling of bone. J Biomed Eng. 1993;15(6):505–9.
38. Pistoia W, van Rietbergen B, Lochmuller EM, Lill CA, Eckstein F, Ruegsegger P. Estimation of distal radius failure load with micro-finite element analysis models based on three-dimensional peripheral quantitative computed tomography images. Bone. 2002;30(6):842–8.
39. Keaveny TM. Biomechanical computed tomography-noninvasive bone strength analysis using clinical computed tomography scans. Ann N Y Acad Sci. 2010;1192:57–65.
40. Nawathe S, Juillard F, Keaveny TM. Theoretical bounds for the influence of tissue-level ductility on the apparent-level strength of human trabecular bone. J Biomech. 2013;46(7):1293–9.
41. Keyak JH, Rossi SA. Prediction of femoral fracture load using finite element models: an examination of stress- and strain-based failure theories. J Biomech. 2000;33(2):209–14.
42. Kelly N, Harrison NM, McDonnell P, McGarry JP. An experimental and computational investigation of the post-yield behaviour of trabecular bone during vertebral device subsidence. Biomech Model Mechanobiol. 2013;12(4):685–703.
43. Rincon-Kohli L, Zysset PK. Multi-axial mechanical properties of human trabecular bone. Biomech Model Mechanobiol. 2009;8(3):195–208.
44. Bousson VD, Adams J, Engelke K, Aout M, Cohen-Solal M, Bergot C, Haguenauer D, Goldberg D, Champion K, Aksouh R, Vicaut E, Laredo JD. In vivo discrimination of hip fracture with quantitative computed tomography: results from the prospective

European Femur Fracture Study (EFFECT). J Bone Miner Res. 2011;26(4):881–93.
45. Macneil JA, Boyd SK. Bone strength at the distal radius can be estimated from high-resolution peripheral quantitative computed tomography and the finite element method. Bone. 2008;42(6):1203–13.
46. Pistoia W, van Rietbergen B, Lochmuller EM, Lill CA, Eckstein F, Ruegsegger P. Image-based micro-finite-element modeling for improved distal radius strength diagnosis: moving from bench to bedside. J Clin Densitom. 2004;7(2):153–60.
47. Varga P, Pahr DH, Baumbach S, Zysset PK. HR-pQCT based FE analysis of the most distal radius section provides an improved prediction of Colles' fracture load in vitro. Bone. 2010;47(5):982–8.
48. Mueller TL, Christen D, Sandercott S, Boyd SK, van Rietbergen B, Eckstein F, Lochmuller EM, Muller R, van Lenthe GH. Computational finite element bone mechanics accurately predicts mechanical competence in the human radius of an elderly population. Bone. 2011;48(6):1232–8.
49. Engelke K, Mastmeyer A, Bousson V, Fuerst T, Laredo JD, Kalender WA. Reanalysis precision of 3D quantitative computed tomography (QCT) of the spine. Bone. 2009;44(4):566–72.
50. Lang TF, Li J, Harris ST, Genant HK. Assessment of vertebral bone mineral density using volumetric quantitative CT. J Comput Assist Tomogr. 1999;23(1):130–7.
51. Li W, Sode M, Saeed I, Lang T. Automated registration of hip and spine for longitudinal QCT studies: integration with 3D densitometric and structural analysis. Bone. 2006;38(2):273–9.
52. Museyko O, Bousson V, Adams J, Laredo J, Engelke K. QCT of the proximal femur-which parameters should be measured to discriminate hip fracture? Osteoporos Int. 2015. doi:10.1007/s00198-015-3324-6.
53. Yang L, Burton AC, Bradburn M, Nielson CM, Orwoll ES, Eastell R, Osteoporotic G. Fractures in men study, distribution of bone density in the proximal femur and its association with hip fracture risk in older men: the osteoporotic fractures in men (MrOS) study. J Bone Miner Res. 2012;27(11):2314–24.
54. Carpenter RD, Saeed I, Bonaretti S, Schreck C, Keyak JH, Streeper T, Harris TB, Lang TF. Inter-scanner differences in in vivo QCT measurements of the density and strength of the proximal femur remain after correction with anthropomorphic standardization phantoms. Med Eng Phys. 2014;36(10):1225–32.
55. Burghardt AJ, Pialat JB, Kazakia GJ, Boutroy S, Engelke K, Patsch JM, Valentinitsch A, Liu D, Szabo E, Bogado CE, Zanchetta MB, McKay HA, Shane E, Boyd SK, Bouxsein ML, Chapurlat R, Khosla S, Majumdar S. Multicenter precision of cortical and trabecular bone quality measures assessed by high-resolution peripheral quantitative computed tomography. J Bone Miner Res. 2013;28(3):524–36.
56. Engelke K, Stampa B, Timm W, Dardzinski B, de Papp AE, Genant HK, Fuerst T. Short-term in vivo precision of BMD and parameters of trabecular architecture at the distal forearm and tibia. Osteoporos Int. 2012;23(8):2151–8.
57. Cody DD, Hou FJ, Divine GW, Fyhrie DP. Short term in vivo precision of proximal femoral finite element modeling. Ann Biomed Eng. 2000;28(4):408–14.
58. Ellouz R, Chapurlat R, van Rietbergen B, Christen P, Pialat JB, Boutroy S. Challenges in longitudinal measurements with HR-pQCT: evaluation of a 3D registration method to improve bone microarchitecture and strength measurement reproducibility. Bone. 2014;63:147–57.
59. Paggiosi MA, Eastell R, Walsh JS. Precision of high-resolution peripheral quantitative computed tomography measurement variables: influence of gender, examination site, and age. Calcif Tissue Int. 2014;94(2):191–201.
60. MacNeil JA, Boyd SK. Improved reproducibility of high-resolution peripheral quantitative computed tomography for measurement of bone quality. Med Eng Phys. 2008;30(6):792–9.
61. Wang X, Sanyal A, Cawthon PM, Palermo L, Jekir M, Christensen J, Ensrud KE, Cummings SR, Orwoll E, Black DM, Osteoporotic Fractures in Men Research, Keaveny TM. Prediction of new clinical vertebral fractures in elderly men using finite element analysis of CT scans. J Bone Miner Res. 2012;27(4):808–16.
62. Graeff C, Marin F, Petto H, Kayser O, Reisinger A, Pena J, Zysset P, Gluer CC. High resolution quantitative computed tomography-based assessment of trabecular microstructure and strength estimates by finite-element analysis of the spine, but not DXA, reflects vertebral fracture status in men with glucocorticoid-induced osteoporosis. Bone. 2013;52(2):568–77.
63. Imai K, Ohnishi I, Matsumoto T, Yamamoto S, Nakamura K. Assessment of vertebral fracture risk and therapeutic effects of alendronate in postmenopausal women using a quantitative computed tomography-based nonlinear finite element method. Osteoporos Int. 2009;20(5):801–10.
64. Orwoll ES, Marshall LM, Nielson CM, Cummings SR, Lapidus J, Cauley JA, Ensrud K, Lane N, Hoffmann PR, Kopperdahl DL, Keaveny TM, Osteoporotic G. Fractures in Men Study, Finite element analysis of the proximal femur and hip fracture risk in older men. J Bone Miner Res. 2009;24(3):475–83.
65. Amin S, Kopperdhal DL, Melton LJ 3rd, Achenbach SJ, Therneau TM, Riggs BL, Keaveny TM, Khosla S. Association of hip strength estimates by finite-element analysis with fractures in women and men. J Bone Miner Res. 2011;26(7):1593–600.
66. Nishiyama KK, Ito M, Harada A, Boyd SK. Classification of women with and without hip fracture based on quantitative computed tomography and finite element analysis. Osteoporos Int. 2014;25(2):619–26.
67. Johannesdottir F, Poole KE, Reeve J, Siggeirsdottir K, Aspelund T, Mogensen B, Jonsson BY, Sigurdsson S, Harris TB, Gudnason VG, Sigurdsson G. Distribution of cortical bone in the femoral neck and hip fracture: a prospective case-control analysis of 143 incident hip fractures; the AGES-REYKJAVIK Study. Bone. 2011;48(6):1268–76.
68. Engelke K, Lang T, Khosla S, Qin L, Zysset P, Leslie WD, Shepherd JA, Shousboe JT. Clinical use of quantitative computed tomography-based advanced techniques in the management of osteoporosis in adults: the 2015 ISCD official positions-part III. J Clin Densitom. 2015;18(3):393–407.
69. Majumdar SR, Leslie WD. Conventional computed tomography imaging and bone mineral density: opportunistic screening or "incidentaloporosis"? Ann Intern Med. 2013;158(8):630–1.
70. Pickhardt PJ, Bodeen G, Brett A, Brown JK, Binkley N. Comparison of femoral neck BMD evaluation obtained using lunar DXA and QCT with asynchronous calibration from CT colonography. J Clin Densitom. 2015;18(1):5–12.
71. Buckens CF, Dijkhuis G, de Keizer B, Verhaar HJ, de Jong PA. Opportunistic screening for osteoporosis on routine computed tomography? An external validation study. Eur Radiol. 2015;25(7):2074–9.
72. Boutroy S, Van Rietbergen B, Sornay-Rendu E, Munoz F, Bouxsein ML, Delmas PD. Finite element analysis based on in vivo HR-pQCT images of the distal radius is associated with wrist fracture in postmenopausal women. J Bone Miner Res. 2008;23(3):392–9.
73. Christen D, Melton LJ 3rd, Zwahlen A, Amin S, Khosla S, Muller R. Improved fracture risk assessment based on nonlinear micro-finite element simulations from HRpQCT images at the distal radius. J Bone Miner Res. 2013;28(12):2601–8.

74. Melton LJ 3rd, Christen D, Riggs BL, Achenbach SJ, Muller R, van Lenthe GH, Amin S, Atkinson EJ, Khosla S. Assessing forearm fracture risk in postmenopausal women. Osteoporos Int. 2010;21(7):1161–9.
75. Nishiyama KK, Macdonald HM, Hanley DA, Boyd SK. Women with previous fragility fractures can be classified based on bone microarchitecture and finite element analysis measured with HR-pQCT. Osteoporos Int. 2013;24(5):1733–40.
76. Vilayphiou N, Boutroy S, Sornay-Rendu E, Van Rietbergen B, Munoz F, Delmas PD, Chapurlat R. Finite element analysis performed on radius and tibia HR-pQCT images and fragility fractures at all sites in postmenopausal women. Bone. 2010;46(4):1030–7.
77. Manske SL, Zhu Y, Sandino C, Boyd SK. Human trabecular bone microarchitecture can be assessed independently of density with second generation HR-pQCT. Bone. 2015;79:213–21.
78. Pahr DH, Schwiedrzik J, Dall'Ara E, Zysset PK. Clinical versus pre-clinical FE models for vertebral body strength predictions. J Mech Behav Biomed Mater. 2014;33:76–83.
79. Zysset P, Pahr D, Engelke K, Genant HK, McClung MR, Kendler DL, Recknor C, Kinzl M, Schwiedrzik J, Museyko O, Wang A, Libanati C. Comparison of proximal femur and vertebral body strength improvements in the FREEDOM trial using an alternative finite element methodology. Bone. 2015;81:122–30.